PROCEEDINGS OF SPIE

Effect of periodicity in the optimization of fine tuned dipolar plasmonic structures for SERS

Henrique Vilhena, Scott G. McMeekin, A. Sheila Holmes-Smith, Graham G. Sharp, Richard M. De La Rue, et al.

SPIE.

Effect of periodicity in the optimization of fine tuned dipolar plasmonic structures for SERS

Henrique Vilhena*[a], Scott G. McMeekin[a], A. Sheila Holmes-Smith[a], Graham G. Sharp[b], Richard M. De La Rue[b], Nigel P. Johnson[b]

[a]School of Engineering and Built Environment, Glasgow Caledonian University, G4 0BA, UK
[b]School of Engineering, University of Glasgow, G12 8QQ, UK

ABSTRACT

Arrays of nanoantennas consisting of plasmonic dipole pairs have been widely used in surface-enhanced Raman spectroscopy (SERS). Fine-tuned structures that can efficiently convert incident electromagnetic energy to excite molecules and provide enhanced detection. However, this tuning mechanism also has its disadvantages. In order to prevent the cross coupling, the distance between each individual element must be increased. This leads to low packing density values which in turn results in a reduction of the overall enhanced Raman signal when these structures are compared to broadly tuned aggregates of particles such as those obtained through metal sputtering or colloidal deposition. In this work we demonstrate through simulations and experimental work that it is possible to increase the reflected signal of an array of nanoantennas by reducing the distance between them in the direction both perpendicular and parallel to the orientation of the incident electric field. It is shown the resonant wavelength shifts in two different spectral directions depending in how the intercell distance was reduced. These resultant shifts can reduce the tuning capabilities of the structures but also can increase the SERS intensity due to close coupling of the dipole pairs. We believe that these results will enable the design and fabrication of structures possessing a greater degree of tunability together with an overall enhanced Raman signal that can rival aggregated SERS substrates.

Keywords: SERS, localized surface plasmon resonance, nanoantennas, electron-beam lithography

1. INTRODUCTION

The use of plasmonic metal nanoparticles as highly tuned nanoantennas for surface-enhanced Raman spectroscopy (SERS) has been the subject of extensive study due to the occurrence of surface plasmon resonances when these particles are irradiated with electromagnetic radiation[1-6]. Different fabrication methods have been used for the development of these structures and in many cases they have been commercially available as reliable and relatively easy to use sensing devices[7-10]. Detecting small amounts of organic compounds using portable and fast devices has diverse applications in a wide range of fields such as security[11], food safety[12] and environmental monitoring[13]. Although gold nanoparticles have lower enhancement values when compared to silver they are less prone to oxidation and show considerable robustness for use in plasmonic sensing[14]. Coupled pairs of nanoparticles such as dipoles[15] and bowties[16] have been widely used due to the formation of highly localized near-field enhancement (so called "hot spots") in these structures as well as to the ability to tune their resonant wavelength to that of the incident Raman wavelength[17,18]. Periodic arrangements of these nanoparticle pairs have high reproducibility and structural reliability and possess very high enhancement values due to the conversion of the irradiating energy at these hot spots[19]. Despite this and, in order to prevent unexpected shifts in the resonant wavelength of these arrays, any cross-talk between these repeating structure is usually minimized which is done by increasing the distance between the unit cells that form these arrays[20]. As the number of nanoparticles per unit area is decreased, however, so will the number of hot spots be reduced and this can lead to low SERS signals. Recent studies[21] have shown that decreasing the interparticle distance will result in an increase of the SERS intensity although results are still lacking in the literature as to the effects that this decrease has upon the resonant wavelength.

*Henrique.Vilhena@gcu.ac.uk; M217, School of Engineering and Built Environment, Glasgow Caledonian University, G4 0BA, UK

Increasing the packing density (the number of particles per unit area) in periodic arrays can be made either by decreasing the distance between the unit cells that constitute these arrays or by increasing the number of particles inside the unit cells. Either of these would result in an increase of the SERS signal but it would also mean that any shifts in the resonance should be accounted for. This effect and the increase in the SERS signal would result in more effective SERS structures.

In this report we show that it is possible to optimize arrays of gold dipole pair nanostructures by carefully controlling their inter-cell distance. Using E-beam lithography we fabricated arrays of repeating dipole pairs on a silica substrate. Measuring their optical response and comparing it with FDTD simulations we show that increasing the packing density can, in turn, result in an increase of the intensity of the reflected light while all resonance shifts can be accounted for. We propose also that the shifts can be used for further tuning. Raman measurements performed over these surfaces after deposition with 1,2-di-4-pyridylethene (BPE) show an increase of the SERS signal that matches the increasing reflected light.

2. METHODOLOGY

A sample containing 500 μm square arrays of repeating dipolar structures was fabricated through a combination of electron-beam lithography, metal deposition and lift-off. Poly(methyl methacrylate) (PMMA) was used as a positive tone resist and was spin-coated over a fused silica substrate. A Vistec Vector Beam 6 electron-beam machine was used for patterning. The sample was developed using a 7:3 isopropanol (IPA) and water solution. Using a vacuum metal evaporator, a 2 nm thick titanium adhesion layer was deposited followed by 30 nm of gold. Lift-off was performed by immersing the sample in warm acetone for 12 hours followed by clean up using IPA and blow drying it with a nitrogen gun. A Hitachi S4700 field emission electron microscope was used for the sample inspection.

The periodicity in each direction was changed for two sets of arrays. In one set the periodicity in the x direction (P_x) was changed from 300 to 400 nm while the distance in the y direction (P_y) was kept at 400 nm. For the other set of arrays the reverse was done: P_y was changed from 300 nm to 400 nm in 20 nm increments while P_y was kept at 400 nm.

Optical characterization of the sample was performed using a white light source, lock-in detection and a Horiba monochromator. Scans were performed from a wavelength of 500 nm up to 1 μm in 2 nm increments. The polarization of the incident electric field was oriented along the dipoles. For each measurement the whole surface of the array was irradiated. The response from the silica substrate without any array was also taken and subtracted from the results. Scans were also performed over a sample containing a uniform layer of 30 nm of gold and these were used to normalize the results.

After optical characterization, the sample was cleaned in a 15% solution of nitric acid and then rinsed in water. It was then submerged in acetone followed by IPA and blow dried with nitrogen. Deposition was performed by drop casting 10μL of a 10 μM solution of 1,2-di-4-pyridylethene (BPE) on ethanol and allowing to dry. Unenhanced measurements of BPE for comparison were taken from a fused silica substrate after 10 μL of a solution with a concentration of 1 mM in ethanol was deposited. Raman and SERS measurements were performed using a WITec alpha300 confocal Raman microscope coupled with an excitation laser source having a wavelength of 785 nm. A 10x microscope objective with numerical aperture of 0.25 was used for all measurements. The incident laser power of 20 mW was measured using a ThorLabs power meter. The spectra were obtained by averaging 10 acquisitions for the SERS measurements and 20 for the unenhanced Raman. The integration time was of 1 s and the background was subtracted from all spectra.

Single unit cells of gold dipole pairs on fused silica with similar dimensions as those fabricated were simulated in Lumerical FDTD Solutions. Results were taken for the values of the periodicity in each direction (P_x and P_y) used in

different arrays in the fabricated sample. By defining the x and y boundaries of the unit cell as periodic, an array of patterns is simulated. The boundaries in the z direction were defined as perfectly matched layers (PML) thus preventing from reflections of the electromagnetic fields. The material properties for the gold and silica were taken from Palik[22]. A planar incident electromagnetic wave was defined with the electric field being oriented along the dipoles.

3. RESULTS AND DISCUSSION

3.1 Structural and optical characterization

Scanning electron microscope (SEM) images obtained of the fabricated structures are shown in Fig. 1. Due to the difficulties inherent to processing at these dimensions, the dipole dimensions are slightly larger than designed. This also accounts for the rounded shape of the dipoles at their edges. The averaged dimensions of the dipoles were taken from the SEM scans. The length of the dipoles was 134 ± 4 nm, their respective width was 51 ± 4 nm and the gap between them was 20 ± 2 nm. The gaps were well formed and no bridging or joining between the structures was observed. The periodicity in both directions was confirmed in all arrays and the extreme values of these can be seen in Fig. 1.
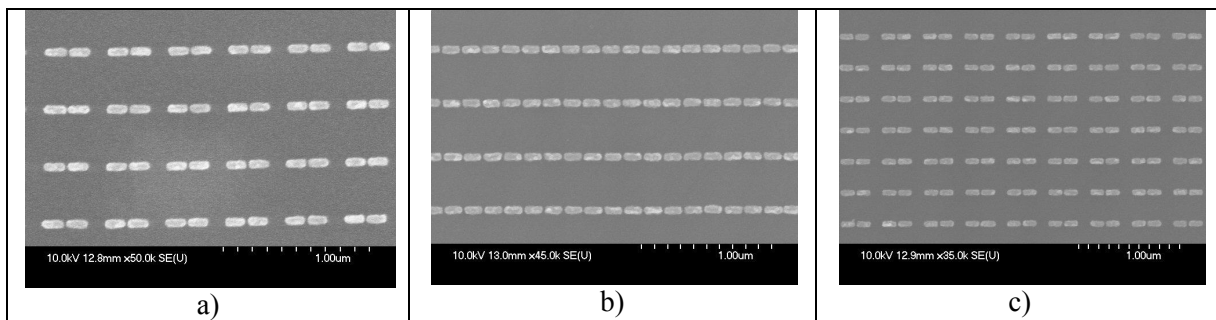
Figure 1 – SEM scans of different fabricated periodic arrays of gold dipole pairs over fused silica: a) array with $P = 400$ nm in both directions, b) array with $P_x = 300$ nm and $P_y = 400$ nm, c) array with $P_x = 400$ nm and $P_y = 300$ nm.

The comparison between the experimental and simulation spectra for the optical response of the nanostructure arrays is shown in Figs. 2 and 3. One can see that there is an offset averaging 80 nm between the simulation and experimental results which could be attributed to deviations in the averaged dimensions as well as the shape of the dipoles. Despite this difference, one can see that the overall behaviour of the simulated and fabricated structures is the same. The position of the resonance is shifted due to the change in periodicity but this change is different for each direction. In the case of the x direction the resonance shifts to longer wavelengths while in the case of the change in the y direction, this shift is now towards shorter wavelengths. Also, this shift is much more dramatic in the x direction. In the experiments the resonant wavelength shifts by 60 nm when P_x is changed when compared to 20 nm for the change in the y direction. The shifts seen here can be attributed to radiative coupling between the distant dipoles and a similar behaviour had already been observed by Cubucku et al. for single dipoles[23].

a)

b)

c)

d)
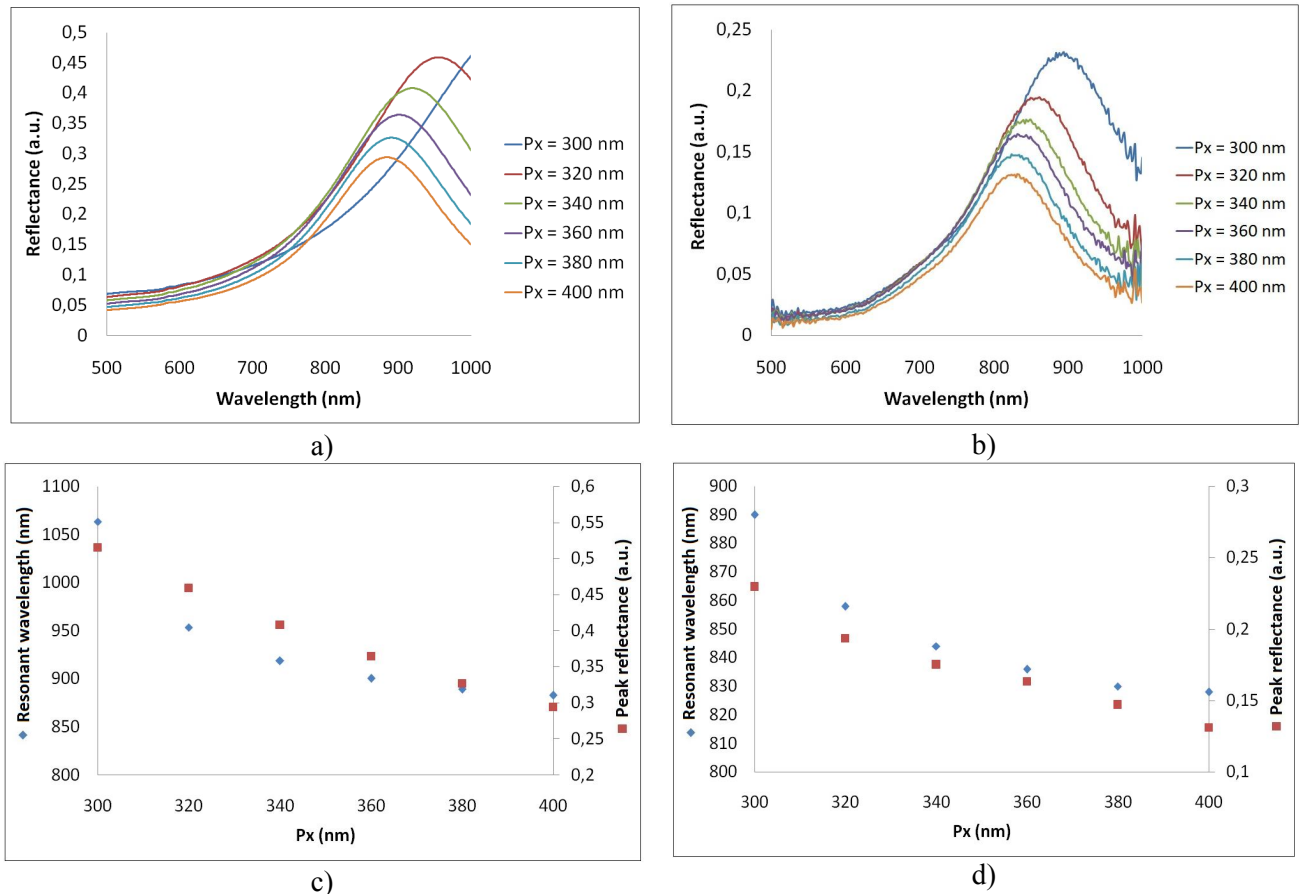
Figure 2 – Comparison between simulation [a) and c)] and experimental [b) and d)] results for the optical responses of different sets of arrays of dipole pairs with $L = 135$ nm, $G = 20$ nm, $W = 51$ nm, $P_y = 400$ nm and P_x changing as indicated.

Looking at the peak reflectance, we can see that it tends to increase in both cases as the periodicity is lowered. This is expected as this value is inversely proportional to the unit cell area[21]. As mentioned before, a higher value of periodicity indicates a lower packing density which would result in a decrease of the reflected light. For both of these structures the reflectance increases with packing density but when the dipoles are brought together in the x direction their resonant wavelength moves significantly to larger values , as can be seen in Fig. 2 and 3. This would limit the application of these devices concerning the excitation wavelength that is used for Raman spectroscopy. In order to use shorter wavelengths one would need to build smaller structures which would entail significant fabrication challenges. When the dipoles are closer together in the y direction, however, the resonance is only slightly shifted and towards shorter wavelengths making these structures more versatile. In particular, the array with $P_y = 300$ nm has a peak reflectance at 808 nm and the array with $P_x = 300$ nm shows a reflectance peak lies further to the red end of the spectrum peaking at 890 nm. This would indicate that, for a 785 nm pump wavelength, the SERS signal would be larger in the former array.
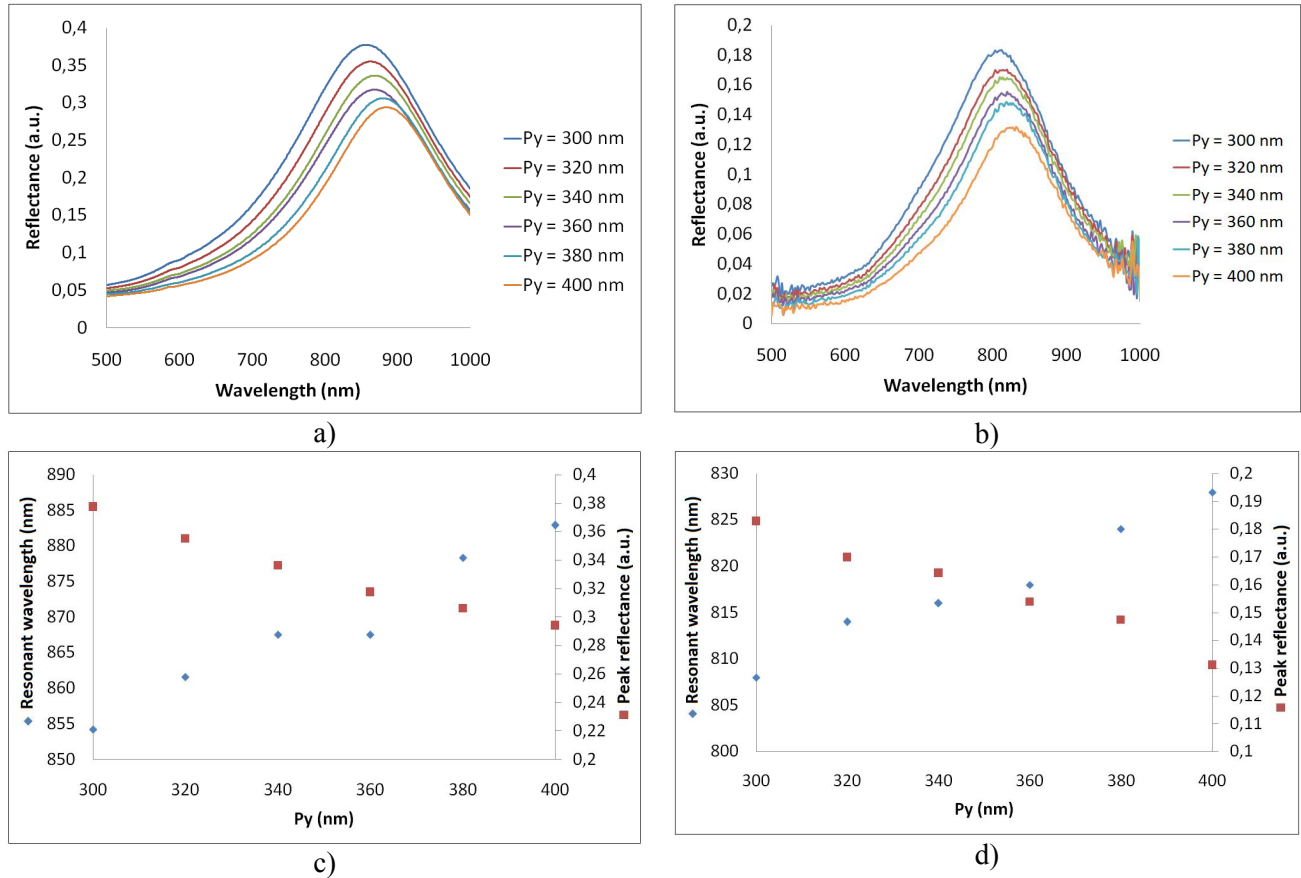
Figure 3 – Comparison between simulation [(a) and (c)] and experimental [(b) and (d)] results for the optical responses of different sets of arrays of dipole pairs with $L = 135$ nm, $G = 20$ nm, $W = 51$ nm, $P_x = 400$ nm and P_y changing as indicated.

3.2 SERS measurements

As indicated in the methodology, the Raman signal was taken from each array and compared with the signal taken from silica. Measurements were done after deposition and drying out of 10 µM of BPE in ethanol on the sample. Fig. 4 compares the Raman signal from the different arrays with the signal obtained over the silica substrate (without nanostructures). One can clearly see that the Raman signal of the BPE is enhanced over each array. Particularly visible are the aliphatic chain vibrations at 1202 cm^{-1} and the double peaks at 1607 cm^{-1} and 1640 cm^{-1} for the C=C and C=N vibrations respectively[24]. All of these correspond to the molecular structure of BPE molecule[25]. The smaller peaks at 1015 cm^{-1} and at 1340 cm^{-1}, which are also attributable to BPE[25], are barely visible above the noise in the unenhanced signal and at the arrays where this enhancement is weaker. One can also observe that the arrays where one of the periodicity values is 300 nm, the enhancement is greater particularly for the case of P_y.

It should be noted that the noise was considerable in all SERS measurements. This arises from the small Raman counts that were available at the incident energy over the arrays. Due to the plasmonic resonances gold nanoparticles are known to convert a considerable part of the absorbed energy into heat. This is a well known issue in these nanostructures[26,27].
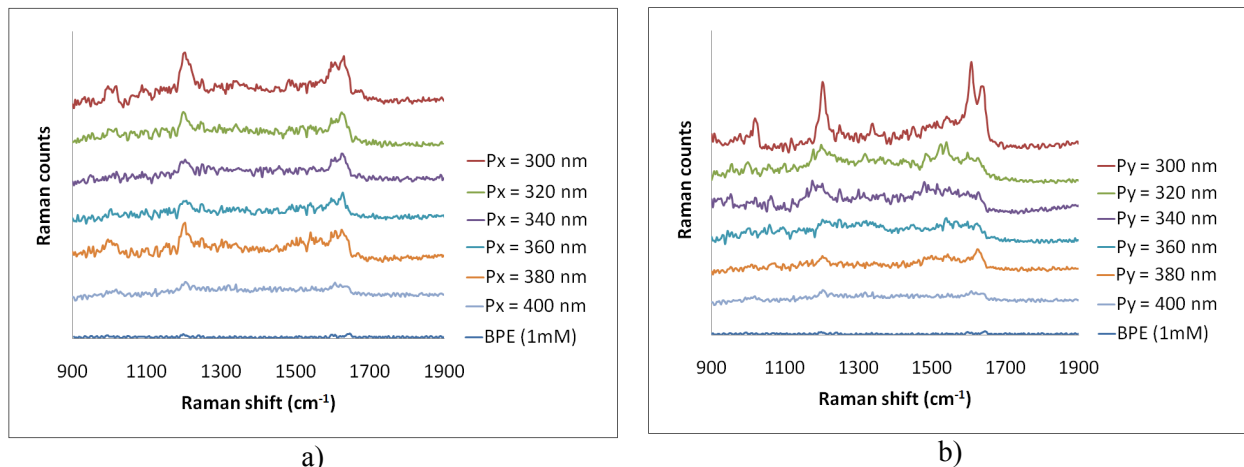
Figure 4 – Comparison between the unenhanced Raman spectrum of BPE and the SERS spectra obtained from different arrays with periodicity values changing in a) the *x* direction directions and b) *y* direction. The unenhanced spectrum was obtained after 10 μL of a 1 mM BPE solution in ethanol was deposited over a silica substrate while the SERS spectra were acquired after the same volume of a 10 μM solution was deposited over the fabricated arrays.

The metal fill factor (*MFF*) is defined as the ratio between the area occupied by the metal and the total area in the unit cell and it is obvious that changing the periodicity results in different values for the *MFF*. A comparison between the SERS results and the reflectance for each array at different values of *MFF* is necessary in order to properly judge the effectiveness of the increase of the packing density within the SERS substrate. Such a comparison would also shed light upon the influence of the changing density of the hot spots since the latter should be proportional to the *MFF*. One should note that the value of *MFF* changes in the same way regardless of the direction according to which the periodicity is changing. The peak at 1202 cm^{-1} was chosen due to its clarity within the background noise. The total SERS intensity (I_{SERS}) for this peak was obtained by integrating it within an interval of 50 cm^{-1} centred at the maximum peak value.

In Fig. 5 we can see that the SERS intensity increases with the increase of the metal fill factor. However, although this behaviour matches the increase of the reflectance in the case of P_y, this does not happen in the *x* direction where the trend of the reflectance does not follow a clear line. Instead, the reflectance at this wavelength rises with lowering periodicity but it starts decreasing again when *MFF* is lower than 10% (P_x lower than 340 nm). This is due to the observed shift in the resonant wavelength. It should be also be noted that, when P_x is smaller than 340 nm, the gaps between each dipole pair will begin to have dimensions comparable to the 20 nm gaps between the dipoles themselves and the structure will start to resemble a long nanowire with periodic gaps as is seen in Fig. 1 b). In order to explain the slower rate of increase for the SERS intensity when $P_x \geq 340$ nm, one could argue that the growth of the resonance with smaller P_x arising from the increase in metal density is being affected by the detuning of the structures to the incident wavelength. However, at P_x values below 340 nm, the structure resembles a nanowire, as mentioned before, and the new small gaps that are formed give rise to additional hot spots which could help explain why the SERS intensity starts increasing at this point.
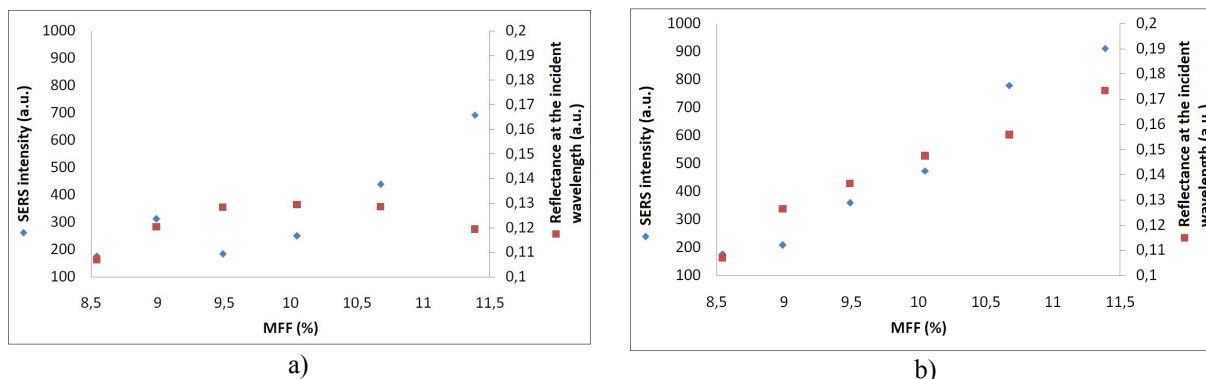
Figure 5 – Comparison between the SERS intensity integrated over the peak centred at 1202 cm^{-1} and the reflectance at the incident excitation wavelength of 785 nm and the change in metal fill factor *MFF* arising from the different values of the periodicity in the *x* (a) and *y* (b) directions.

Taking the I_{SERS} values from Fig, 5 and the Raman intensity (I_R) integrated over the same interval in the unenhanced spectrum in Fig. 4, the enhancement factor (*EF*) can be calculated using the formula[28].

$$EF = \frac{I_{SERS}}{I_R} \times \frac{N_R}{N_{SERS}},\tag{1}$$

where N_R is number of molecules that are Raman scattered in the unenhanced measurement and N_{SERS} is the number of molecules that are adsorbed onto the dipoles. For the unenhanced measurement, the total volume within which the analyte molecules are Raman scattered can be compared to a cylinder shape with height $H = (16\lambda f^2)/(\pi d^2)$ and diameter[26,29,30] $D = (4\lambda f)/(\pi d)$ where *f* is the focal length of the pump laser beam and *d* is the diameter of the unfocused beam. From this volume, the concentration of 1mM and Avogadro's number it was easy to estimate the number of molecules from the unenhanced measurement to be 8.48×10^{15}. For a concentration of 10 mM the surface density μ of BPE can be estimated to be[31] 1×10^{-12} mol·mm^{-2}. From this the number of molecules that are attached to the metal within the laser spot can be estimated calculated using the following formula:

$$N_{SERS} = \mu N_A \pi r^2 MFF.\tag{2}$$

In this case N_A is Avogadro's number, and *r* is the laser spot radius given by[26] $r = (1.22\lambda)/2NA$, where *NA* is the numerical aperture of the objective lens. Based on these considerations the enhancement factor felt by a single molecule was calculated to be of the order of 10^6.

4. CONCLUSIONS

We have showed that arrays of repeating gold dipole pairs on silica behave differently when their periodicity is changed in two different directions. In particular, it was observed that changing the periodicity in the *x* direction results in a red shift of the structures' resonant wavelength at a rate of 3 nm per 5nm of the periodicity. The expected rise of the SERS intensity due to the higher density of hot spots as well as exposed metal is affected by this shift as the array becomes further out of tune to the incident wavelength. In order to compensate for this, smaller structures would have to be built so that their resonance would match the excitation wavelength but this would greatly increase the challenges with the e-beam fabrication process[32]. It was also pointed out that, below a certain threshold, the gaps between each dipole pair will acquire dimensions similar to those of the gaps within the pairs and the structure will start to resemble a nanowire with periodic gaps. This would add additional hot spots within these gaps which could be the reason for the observed increase of the SERS intensity. When changing the periodicity in the *y* direction it is seen that the resonant wavelength blue shifts

by a smaller rate of 1 nm per 5 nm of the periodicity. This suggests that smaller distances in this direction would not just result in an increase of the number of hot spots per unit area but also a greater versatility while tuning these structures to the excitation wavelength. In this work it was found that an array of dipole pairs at a distance of 300 nm in the y direction with a resonance located 20 nm away to the incident laser beam can provide high SERS intensity values with a single molecule enhancement factor of 10^6. Although this value is not as high as those seen for structures with smaller gaps sizes[3], we could expect to achieve higher intensity and enhancement values by fabricating structures more accurately tuned to the incident wavelength and by further reducing the periodicity in the y direction. We believe that this will enable development of ever more sensitive and reliable SERS devices.

ACKNOWLEDGEMENTS

REFERENCES

[1] Cubukcu, E., Smythe, E. J., Diehl, L., Crozier, K. B. and Capasso, F., "Plasmonic Laser Antennas and Related Devices," IEEE J. Quantum Elect. 14(6), 1448–1461 (2008).

[2] Cialla, D., März, A., Böhme, R., Theil, F., Weber, K., Schmitt, M. and Popp, J., "Surface-enhanced Raman spectroscopy (SERS): Progress and trends," Anal. Bioanal. Chem. 403(1), 27–54 (2012).

[3] Kleinman, S. L., Frontiera, R. R., Henry, A.I., Dieringer, J. and Van Duyne, R. P., "Creating, characterizing, and controlling chemistry with SERS hot spots," Phys. Chem. Chem. Phys.: PCCP 15 (1), 21-36 (2013).

[4] Vilhena, H., McMeekin, S. G., Holmes-Smith, A. S. and Johnson, "Optimization of dipole structures for detection of organic compounds," N. P. s.l. : Proc. SPIE 9502, 950212 (2015).

[5] Wang, A. and Kong, X., "Review of Recent Progress of Plasmonic Materials and Nano-Structures for Surface-Enhanced Raman Scattering," Materials 8(6), 3024–3052 (2015).

[6] Li, J. F., Zhang, Y. J., Ding, S. Y., Panneerselvam, R. and Tian, Z. Q. "Core− Shell Nanoparticle-Enhanced Raman Spectroscopy," Chem. Rev. (2017).

[7] Sarau, G., Lahiri, B., Banzer, P., Gupta, P., Bhattacharya, A., Vollmer, F. and Christiansen, S., "Enhanced Raman Scattering of Graphene using Arrays of Split Ring Resonators," Advanced Optical Materials 1(2), 151–157, (2013).

[8] Taylor, R. W., Esteban, R., Mahajan, S., Aizpurua, J. and Baumberg, J. J., "Optimizing SERS From Gold Nanoparticle Clusters: Addressing The Near-Field By An Embedded Chain Plasmon Model," J. Phys. Chem. C. 120(19), 10512-10522 (2016).

[9] Sun, X. and Li, H., "A Review : Nanofabrication of Surface-Enhanced Raman Spectroscopy (SERS) Substrates," Curr. Nanosci. 12(2), 175–183 (2016).

[10] Cerjan, B., Yang, X., Nordlander, P. and Halas, N. J., "Asymmetric aluminum antennas for self-calibrating surface-enhanced infrared absorption spectroscopy," ACS Photonics 3(3), 354-360 (2016).

[11] López-López, M. and Carmen G., "Infrared and Raman spectroscopy techniques applied to identification of explosives," Trac-Trend. Anal. Chem. 54, 36-44 (2014).

[12] Wijaya, W., Pang, S., Labuza, T. P. and He, L., "Rapid Detection of Acetamiprid in Foods using Surface-Enhanced Raman Spectroscopy (SERS)," J. Food Sci. 79(4), 1–5 (2014).

[13] Qu, X., Alvarez, P. J. J. and Li, Q., "Applications of nanotechnology in water and wastewater treatment," Water Res. 47(12), 3931–3946 (2013).

[14] Crozier, K. B., Member, S., Zhu, W., Wang, D., Lin, S., Best, M. D. and Camden, J. P., "Plasmonics for Surface Enhanced Raman Scattering : Nanoantennas for Single Molecules," IEEE J. Quantum Elect. 20(3), 152-162 (2013).

[15] Kessentini, S., Barchiesi, D., D'Andrea, C., Toma, A., Guillot, N., Di Fabrizio, E., Fazio, B., Marago, O. M., Gucciardi, P. G. and Lamy De La Chapelle, M., "Gold dimer nanoantenna with slanted gap for tunable LSPR and improved SERS," J. Phys. Chem. C., 118(6), 3209–3219 (2014).

[16] Chao, B. K., Lin, S. C., Nien, L. W., Li, J. H. and Hsueh, C. H., "Effects of corner radius on periodic nanoantenna for surface-enhanced Raman spectroscopy," J. Opt-UK 17(12), 125002 (2015).

[17] Fischer, H., and Martin, O. J. F., "Engineering the optical response of plasmonic nanoantennas," Opt. Express 16(12), 9144–54 (2008).

[18] Wissert, M. D., Schell, A. W., Ilin, K. S., Siegel, M. and Eisler, H. J., "Nanoengineering and characterization of gold dipole nanoantennas with enhanced integrated scattering properties," Nanotechnology 20(42), 425203 (2009).

[19] Chen, T., Li, S. and Sun, H., "Metamaterials application in sensing," Sensors 12(3), 2742–2765 (2012).

[20] Zhang, W., Fischer, H., Schmid, T., Zenobi, R. and Martin, O. J. F., "Mode-Selective Surface-Enhanced Raman Spectroscopy Using Nanofabricated Plasmonic Dipole Antennas," J. Phys. Chem. C. 113(33), 14672–14675 (2009).

[21] Wei, S., Zheng, M., Xiang, Q., Hu, H. and Duan, H., "Optimization of the particle density to maximize the SERS enhancement factor of periodic plasmonic nanostructure array," Optics Express 24(18), 20613-20620 (2016).

[22] Palik, E. D. [Handbook of Optical Constants of Solids], (1998).

[23] Cubukcu, E., Smythe, E. J., Diehl, L., Crozier, K. B. and Capasso, F., "Plasmonic Laser Antennas and Related Devices," IEEE J. Sel. Top. Quant. 14(6), 1448–1461 (2008).

[24] Lin-Vien, D., Colthup, N. B. , Fateley, W. G. and Grasselli, J. G. [The Handbook of Infrared and Raman Characteristic Frequencies of Organic Molecules], Elsevier, (1991).

[25] Khaywah, M. Y., Jradi, S., Louarn, G., Lacroute, Y., Toufaily, J., Hamieh, T. and Adam, P. M., "Ultrastable, uniform, reproducible, and highly sensitive bimetallic nanoparticles as reliable large scale SERS substrates," J. Phys. Chem. 119(46), 26091-26100 (2015).

[26] Álvarez-Puebla, R. A., "Effects of the excitation Wavelength on the SERS spectrum,". J. Phys. Chem. Lett. 3(7), 857–866 (2012).

[27] Coppens, Z. J., Li, W., Walker, D. G. and Valentine, J. G., "Probing and controlling photothermal heat generation in plasmonic nanostructures," Nano Lett. 13(3), 1023–1028 (2013).

[28] Le Ru, E. C., Blackie, E., Meyer, M. and Etchegoin, P. G., "Surface Enhanced Raman Scattering Enhancement Factors: A Comprehensive Study,". J. Phys. Chem. C. 111(37), 13794–13803 (2007).

[29] Smith, E. and Dent, G. [Modern Raman Spectroscopy: A Practical Approach], John Wiley & Sons, (2005).

[30] Lin, W. C., Huang, S. H., Chen, C. L., Chen, C. C., Tsai, D. P. and H. P. Chiang, "Controlling SERS intensity bytuning the size and height of a silver nanoparticle array," Appl. Phys. A-Mater. 101(1), 185–189 (2010).

[31] Xu, C. H., Xie, B., Liu, Y.J., He, L.B. and Han, M., "Optimizing surface-enhanced Raman scattering by template guided assembling of closely spaced silver nanocluster arrays," E. P. J. D. 52(1), 111-114 (2009).

[32] Ed. Rai-Choudhuri, P. [SPIE Handbook of Microlithography, Micromachining and Microfabrication - Volume 1: Microlithography], SPIE, (2000).